"Enhanced Wellbore Stabilization and Reservoir Productivity with Aphron Drilling Fluid Technology"

QUARTERLY PROGRESS REPORT

April 1 – June 30, 2004

by

Fred Growcock

Issued July, 2004

DOE Award Number DE-FC26-03NT42000

MASI Technologies *LLC*
5950 N. Course Dr.
Houston, Texas 77072

DISCLAIMER

ABSTRACT

During this third Quarter of the Project, three of the tasks of Phase I were completed and the remaining tasks were either initiated or continued. All of these tasks focus on the behavior of micro-bubbles in aphron drilling fluids. The tasks that were completed include (a) Fluid Density - investigate the effects of pressure, temperature and composition on the survivability of aphrons; (b) Aphron Visualization – evaluate and utilize various methods of monitoring and measuring aphron size distribution; and (c) Pressure Transmissibility – determine whether aphron seals created in fractures and pore throats reduce fracture propagation.

Highlights of these three projects included the determination that properly designed aphrons are stable enough to survive repeated compression and decompression up to at least 1,000 psi. In addition, although the rheology of the aphron drilling fluid dominates its flow properties in unconsolidated sands – rate of invasion and pressure transmissibility are significantly lower than for any conventional drilling fluid – aphrons themselves can further reduce invasion rate and pressure transmissibility. Finally, direct optical measurement of the aphrons, coupled with image analysis, appears to be the most accurate and efficient way to determine bubble size distribution. Work on the kinetics of air loss from aphrons is continuing, and preliminary work has been carried out in four new task areas: in-situ (elevated pressure and temperature) visualization, aphron shell hydrophobicity, sealing of permeable media and sealing of fractured media.

Several opportunities presented themselves to share the latest aphron drilling fluid technology developments with potential clients, including presentation of papers at conferences in Houston and Venezuela; working exhibit booths at OTC in Houston and the DEA Workshop in Galveston; attendance of the Annual Review of the DOE-sponsored drilling research projects in Tulsa, OK; and presentation of project updates to the management of M-I SWACO and ActiSystems, Inc. Finally, aphron drilling fluids were featured in the Technology Section of the May issue of the ***Journal of Petroleum Technology***.

TABLE OF CONTENTS

LIST OF FIGURES

INTRODUCTION

Aphron drilling fluids are thought to seal permeable zones by virtue of their very high low-shear rheology and the unique sealing capability of specially designed microbubbles, or "aphrons".[1] These drilling fluids were developed as a more economical and safer alternative to underbalanced drilling. Air is entrained during normal mixing operations – eliminating the need for gas injectors and pumps – at such a low concentration that, under downhole conditions, it does not affect the fluid density significantly.

Aphrons are thought to consist of a core of air enveloped by a protective shell composed of multiple layers of surfactants and polymers.[2] The outer part of the hypothesized structure consists of a surfactant bi-layer that renders the aphron water-wet and, therefore, compatible with the continuous aqueous phase. However, it is also claimed that the outermost surfactant layer in the bi-layer may be shed when aphrons are forced together in a pore throat or near a fracture tip.[1] Under these conditions, aphrons could acquire some oil-wetting character that would permit them to agglomerate without coalescing and seal off the opening without wetting the walls; thus, when the well is put on production, only a low pressure differential is necessary to push the aphron agglomerate into the wellbore.

Neither the structure of the aphron nor its physicochemical properties have been validated sufficiently for the technology to be widely accepted. Acceptance of this novel technology and the consequent reduction in drilling costs would be facilitated greatly by a systematic and thorough evaluation of the structure and behavior of aphron drilling fluids downhole.

The objectives of this project are threefold: (a) develop a comprehensive understanding of how aphrons behave at elevated pressures and temperatures; (b) measure the ability of aphron drilling fluids to seal permeable and fractured formations under simulated downhole conditions; and (c) determine the role played by each component of the drilling fluid.

The Project is divided into two phases. Phase I (Year 1) is focused on developing evidence for the ways in which aphrons behave differently from ordinary surfactant-stabilized bubbles, particularly how they seal permeable and micro-fractured formations during drilling operations. Key properties to be investigated include the effects of pressure on bubble size, the oil-wetting/water-wetting nature of the aphron surface under dynamic conditions, and the nature of aphron seals in fractures and pore networks. Initial sealing and formation damage tests also will be carried out, using lab-scale apparati designed to simulate permeable and micro-fractured environments. Phase II (Year 2) focuses on sealing and formation damage testing of aphron drilling fluids, including scale-up tests under simulated downhole drilling conditions, so as to furnish irrefutable evidence for the validity of this technology and provide field-usable data.

The current schedule of tasks is provided in Figure 1.

Figure 1. Schedule of Tasks to be Performed in Aphron Drilling Fluid Project

	2003	2004				2005		
Task	4th Q	1st Q	2nd Q	3rd Q	4th Q	1st Q	2nd Q	3rd Q
I. Physical Characterization of Aphrons								
1.1 Aphron Visualization	X	X	X					
1.2 Fluid Density	X	X	X*					
1.3 Aphron Air Diffusivity	X	X	X	X**				
2.1 In Situ Visualization			X	X				
2.2 Pressure Transmissibility	X	X	X					
2.3 Aphron Shell Hydrophobicity			X	X				
3.1 Sealing of Permeable Media			X	X				
3.2 Sealing of Fractured Media			X	X				
II. Characterization of Aphron Drilling Fluids								
1.1 Lab Tests Leak-Off/Return Perm					X	X	X	
1.2 Field-Sim Tests Leak-Off/Return Perm							X	X
2.1 Flow Sim through & Sealing Fractures					X	X	X	X
2.2 Fracture Re-Opening Tests						X	X	X

* 1-Month Extension Proposed April 1, 2004
** 2-Month Extension Proposed June 30, 2004

The tasks marked with a red **X** were completed during the 2nd Quarter of 2004. An extension is being requested for the Aphron Air Diffusivity project. The other four tasks in Phase I were begun during this Quarter; all of these are scheduled to be completed by the end of Phase I, i.e. the end of the 3rd Quarter of 2004.

EXECUTIVE SUMMARY

All eight tasks in Phase I, which focus on the behavior of aphrons, were in progress during this 3rd Quarter. Three of these tasks were completed: 1.1 Aphron Visualization – evaluation of potential methods for measurement of bubble size distribution (BSD), especially Acoustic Bubble Spectroscopy (ABS), in aphron drilling fluids; 1.2 Fluid Density – investigation of the effect of pressure on the survivability of aphrons; and 2.2 Pressure Transmissibility – evaluation of the ability of aphron drilling fluids to reduce pressure transmission in permeable media. Another task -- 1.3 Aphron Air Diffusivity – was found to need some additional work, and a 1-month extension has been requested. This task involves determination of the rate of loss of air from aphrons during pressurization. A technique thought to be very promising, namely measurement of dissolved oxygen in the bulk fluid, was found to be wanting; an optical imaging method is being used instead with good success.

Despite delays caused by ABS software problems, the Aphron Visualization task (# 1.1) was completed ahead of schedule. Additional work will be carried out at elevated pressure under task # 2.1. The results indicate that it is possible to correlate BSD derived from ABS data with BSD determined via conventional laser light scattering. However, the best method by far is direct optical imaging of the bubbles, which must be carried out in a HTHP vessel thin enough to admit light and enable direct visual observation. In addition, a locally available Environmental Scanning Electron Microscope has been checked out and appears to be suitable for *in situ* visualization of the sealing of pore networks.

The Fluid Density task (# 1.2) revealed that aphrons can survive repeated compression / decompression cycles up to at least 7 MPa (1000 psig). The technique involves measurement of the degree of hysteresis in the gas volume after each depressurization to ambient conditions. Essentially the same gas volume is recovered immediately after each depressurization step. Examination of the behavior of the systems after each pressurization step yielded another surprise: the bubbles do not decrease in volume as much as predicted by the ideal gas law, i.e. the bubbles appear to resist pressurization. However, the discrepancy can also be explained by loss of some air during handling of the mud sample. Investigation of this phenomenon is continuing.

The Aphron Air Diffusivity task (# 1.3) encountered problems related to the method employed to determine rate of loss of air from aphrons. Monitoring of dissolved oxygen had been chosen as a promising technique, but it was learned that components in the drilling fluid react very rapidly with dissolved oxygen and preclude accurate measurement of the rate of diffusion of air. Direct optical imaging of the fluid, coupled with bubble size analysis, appears to be very promising. However, additional time is required to carry out the prescribed tests, which cover the effects of pressure, temperature and chemical composition on the rate of loss of air from aphrons.

Lastly, the Pressure Transmissibility task (# 2.2) revealed that the base fluid in APHRON ICS™ fluids gives significantly larger pressure loss (or, for a fixed pressure drop, lower flow rate) in long conduits than does any other conventional high-viscosity drilling fluid. Similarly, if flow is restricted or stopped, APHRON ICS™ fluids (at a fixed wellbore pressure) generate significantly lower downstream pressures than do other muds. The same phenomena are evident in permeable

sands. Furthermore, in permeable sands of moderate permeability (up to at least 8 darcy), aphrons themselves slow the rate of fluid invasion and increase the pressure drop across the sands. Aphrons move more rapidly through the sands than does the base fluid, enabling them to form a seal ahead of the fluid front.

Preliminary work has also begun on all of the other tasks in Phase I of this project:

2.1 *In situ* Visualization

2.3 Aphron Shell Hydrophobicity

3.1 Sealing of Permeable Media

3.2 Sealing of Fractured Media

Initial literature searches and assessment of appropriate test methods were completed for these four tasks. Furthermore, for the Aphron Hydrophobicity task, a method has been devised that is expected to enable aphrons to be compressed, thus enabling measurements of cohesion and adhesion sticking coefficients. For the *In situ* Visualization task, a high-pressure high-temperature circulating system (20.7 MPa, or 3000 psi, and 121 ^{o}C, or 250 ^{o}F) is nearly complete and is being modified with a viewing port that will enable simultaneous ABS and optical imaging. Finally, for the Sealing tests, construction of a triaxial loading core leak-off tester is essentially complete and will be able to be run at pressures up to 17 MPa (2500 psi) and 177 ^{o}C (350 ^{o}F).

Several opportunities presented themselves to share the latest aphron drilling fluid technology with potential clients. These included the following:

- Presented paper # AADE-04-DF-HO-18, "Applications of Novel Aphron Drilling Fluids," at AADE 2004 Drilling Fluids Conference, Houston, Texas, April 6-7.
- Presented update of Project to M-I SWACO R&D management, Houston, Texas, April 1.
- Presented update of Project to ActiSystems at M-I SWACO, Houston, Texas, April 20.
- Worked exhibit booth at *Offshore Technology Conference*, Houston, Texas, May 3-6.
- Aphron technology featured in Technology Applications section of May, 2004 issue of ***Journal of Petroleum Technology***.
- Attended *Tulsa University Drilling Research Program/Advanced Cuttings Transport Study* Annual Review, Tulsa, OK, May 10, 11.
- Presented paper entitled, "Development of Aphron Drilling Fluids," at *SEFLU y CEMPO*, Margarita Is, Venezuela, May 24-28.
- Worked exhibit booth and attended a few presentations at *DEA Workshop*, Galveston, Texas, June 22 & 23.

EXPERIMENTAL APPROACH

The methodologies used for the current tasks are detailed below:

Aphron Visualization

Acoustic bubble spectroscopy (ABS) was evaluated to determine its suitability for measuring bubble size distribution (BSD) in aphron drilling fluids; two conventional methods were used for reference: photomicrography and laser light scattering. To obtain a quantitative comparison, a mud was formulated that is representative of the APHRON ICS™ mud system, yet transparent to light:

Component	Concentration	Mixing Time
FloVis Plus	8.6 g/L (3 lb/bbl)	2 min
50% NaOH	to pH 10	
Blue Streak	2.9 g/L (1 lb/bbl)	1 min
EMI-779	1.4 g/L (0.5 lb/bbl)	1 min
EMI-780	1.4 g/L (0.5 lb/bbl)	2 min

By contrast, the Super Enhanced APHRON ICS™ mud system has the following composition:

Component	Concentration	Mixing Time
Soda Ash	8.6 g/L (3.0 ppb)	5 min
X-CIDE 102	0.05% v/v	3 min
ACTIVATOR II	5.8 g/L (2.0 ppb)	2 min
GO-DEVIL II	14 g/L (5.0 ppb)	2 min
ACTIVATOR I	14 g/L (5.0 ppb)	2 min
ACTIGUARD	2.9 g/L (1.0 ppb)	2 min
BLUE STREAK	2.9 g/L (1.0 ppb)	1 min
EMI-779	1.4 g/L (0.5 ppb)	1 min
EMI-780	1.4 g/L (0.5 ppb)	2 min
EMI-802	0.7 g/L (0.25 ppb)	2 min

A schematic of the ABS system is shown in Figure 2, while the equipment used for photomicrography is shown in Figures 3 and 4, and for laser light scattering in Figure 5. The mud samples employed were Transparent APHRON ICS™ with varying air concentration and shear history.

Figure 2. Configuration of Dynaflow Acoustic Bubble Spectrometer[3]

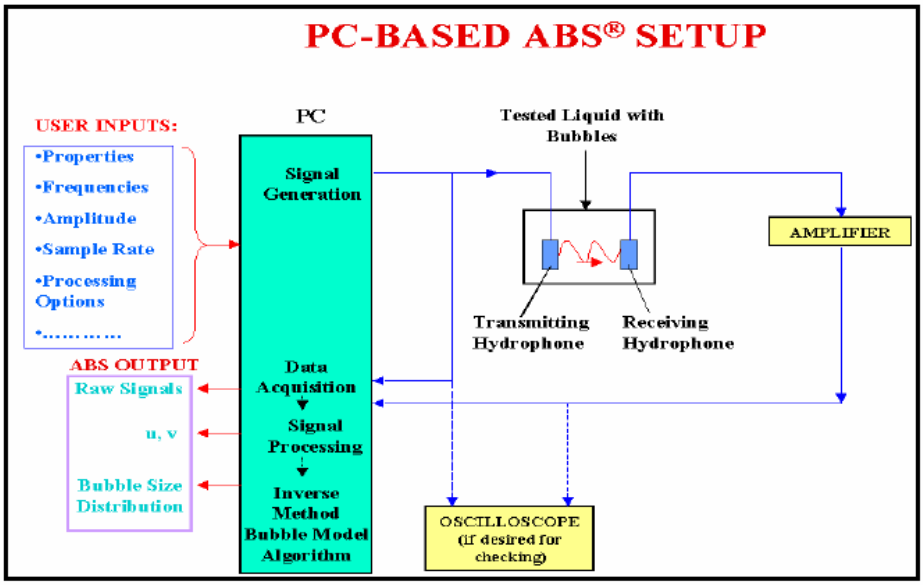

Figure 3. Microscope

Figure 4. Glass Sight Flow Viewing Cell

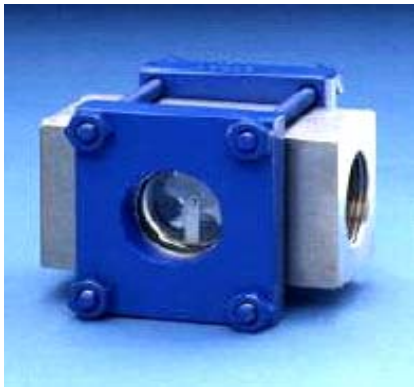

Figure 5. Coulter Laser Light Scattering System

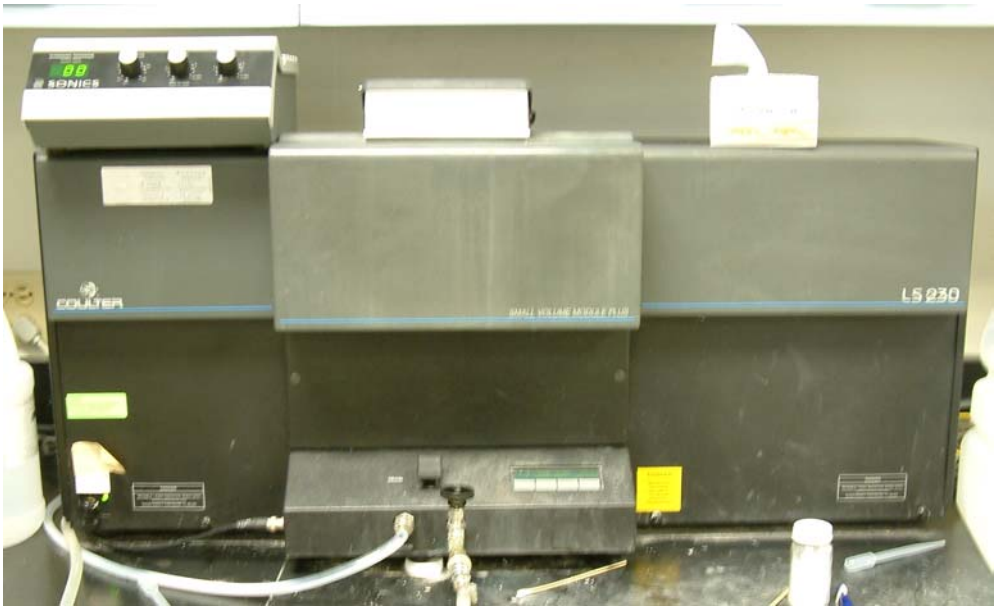

Fluid Density

An Isco pump (used to generate pressure and monitor volume changes of the fluid) was utilized to drive a floating piston in a 500-mL cylinder to which a pistonless 500-mL cylinder was connected. The mud sample subjected to the pressure ramp was almost 1000 mL in volume. Later, the apparatus was modified to reduce the error introduced by air in the plumbing system. The new system was constructed and calibrated, and a few tests were performed. However, a deaerated mud sample still showed, at best, 1 to 2 % undissolved air.

The original intent of this project was to determine if aphrons can survive pressurization to at least 6.9 MPa (1000 psia). For a mud sample of 1000 mL which contains 15% air (aphrons), or 150 mL air, pressurization itself (with no loss of air to the surrounding mud) would reduce the volume of air to 2.25 mL (0.225%). The air that might be "lost" during pressurization is assumed to leak through the aphron shell and dissolve in the mud matrix. Thus, the experimental apparatus must be able to generate distinguishable results between the case where no air is lost vs

all air is lost, i.e. ΔV_0 = 147.8 mL (no loss of air) vs ΔV_{100} = 150 mL (all air is lost). That should be feasible. However, the air trapped in the plumbing at the beginning of a test would generate a ΔV of 10 to 20 mL. Thus, ΔV_0^{Corr} = 157.8 to 167.8 mL and ΔV_{100}^{Corr} = 160 to 170 mL. Since the uncertainty in the trapped air volume (~ 10 mL) is more than four times the expected maximum volume difference ($\Delta V_{100} - \Delta V_0$ = 2.25 mL), the test was completely revamped.

First, rather than measure the volume change during compression, it was decided to investigate the hysteresis effect on the APHRON ICS™ mud after each compression/decompression cycle.

Second, the system was modified by adding a vacuum pump and the associated tubing, fittings and a valve, and utilizing a second floating piston cell (instead of the pistonless accumulator cell) as a filling station for the sample cell. The experimental set-up is shown in Figure 6.

Figure 6. Fluid Density Apparatus

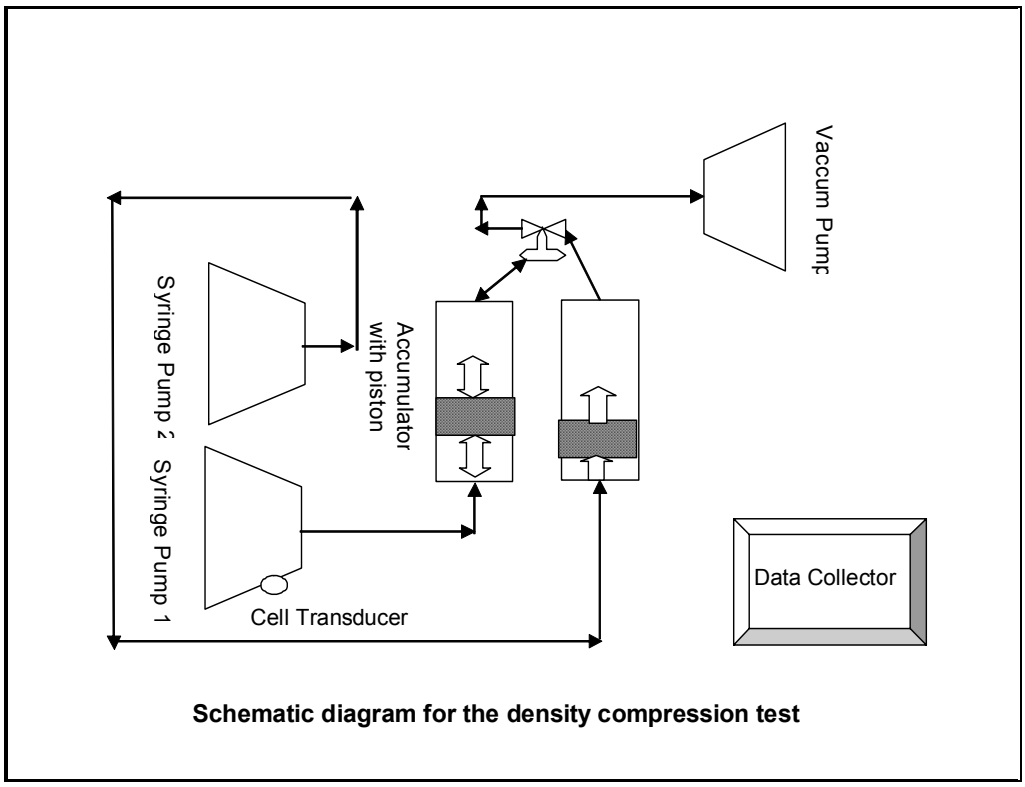

This reduced the active mud volume to about 500 mL (the volume of the sample cell).

The pressure was varied cyclically, by first increasing the pressure for 1.5 minute to the desired value (100 psig, 200 psig and so on up to 1000 psig, in increments of 100 psig, or 0.69 MPa), then decreasing the pressure after each step over a period of 1.5 minutes down to a nominal pressure of 0 psig (actually closer to 10 psig). We noticed that for each cycle, during the depressurizing step the air that was first compressed during the pressurizing step was not all coming back. We thought that this effect was probably due to the short time between the steps, so the time between the steps after that was increased to 10 minutes.

Although in most cases, the volume readings at the end of each cycle were similar to the original volume, no systematic pattern emerged from the volume vs pressure readings. It was determineed that the erratic nature of the readings was likely caused by stick/slip of the floating piston in the accumulator cell, perhaps exacerbated by blow-by of air. To minimize these problems, the piston was redesigned several times and ultimately was fitted with two polyurethane gaskets energized by Viton O-rings. Then the bore of the cylinder was honed, and powdered household lubricating graphite was used to reduce stick-slip further.

The results using that cell were significantly improved, generating relatively stable and monotonically changing volume vs pressure readings.

Aphron Air Diffusivity

To measure the rate of loss of air from aphrons, it was initially postulated that this could be monitored by measuring the rate of increase of Dissolved Oxygen (DO) in the surrounding aqueous medium. Thus, it was necessary to learn the principles of operation of various DO probes, their accuracy and reproducibility, methods of using them, and their limitations, e.g. effect of pressure. Then a vessel was constructed to accommodate a suitable DO probe and enable measurements of DO at elevated pressures and temperatures.

Finally, initial experiments were run at ambient pressure and slightly above to evaluate the potential for DO to serve as an indicator of air loss from aphrons. After a number of DO probes were tried and discarded as inadequate for technical or mechanical reasons, a FOXY probe

(OceanOptics) was found to be the most likely candidate. Figure 7 shows the system configuration that was most recently employed.

Figure 7. FOXY Dissolved Oxygen System for Air Diffusivity Tests

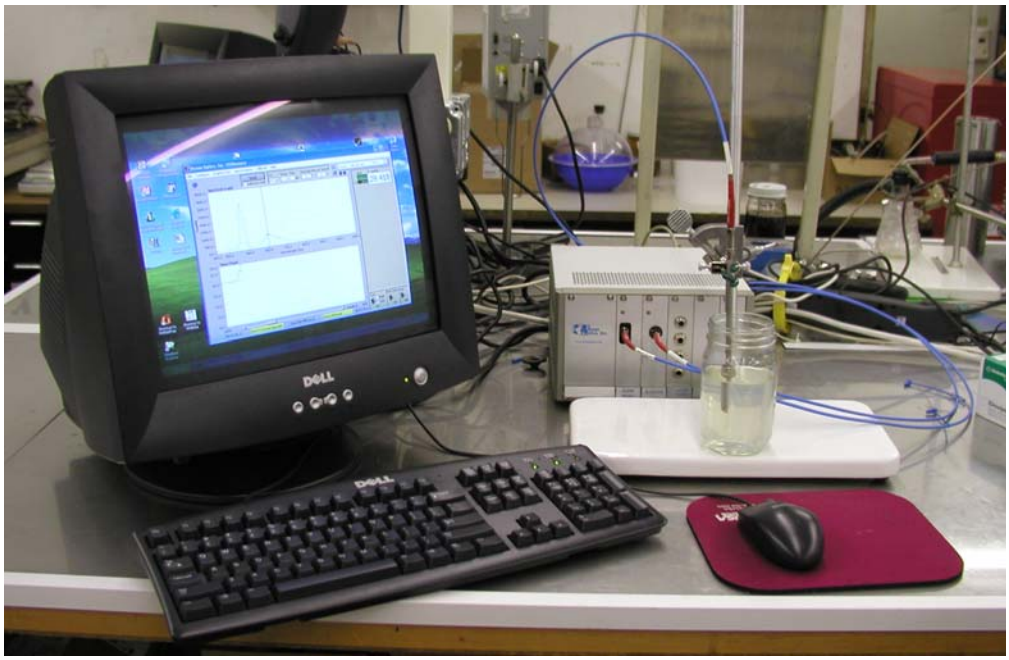

However, as described in the Results section, DO was found to be unacceptable. In the aftermath of that evaluation, optical imaging was chosen as the method to be used for monitoring the rate of loss of air from aphrons. However, the glass sight flow cell shown in Figure 4 was found to be unsuitable for looking at whole drilling fluids, inasmuch as the depth of the opaque fluids is too great to admit sufficient light for proper viewing. Although the lighting problem is minimized by using the transparent version of the APHRON ICS™ fluid, uncertainty in the depth of the bubbles creates a large uncertainty in bubble size determination. Furthermore, some tests need to be carried out with the standard (opaque) mud. Consequently, a new viewing cell was designed and constructed to provide a variable fluid reservoir depth (as shallow as 2 mm). This new microscope cell, made of steel with ½" polycarbonate windows, promises to be useful to pressures of as much as 4,000 psi. Photos of the cell are shown in Figure 8.

Figure 8. Variable-Reservoir-Depth Polycarbonate Viewing Cell

Front View of Cell

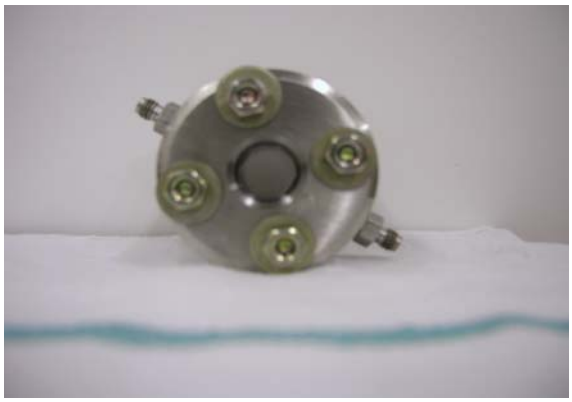

Side View of Cell

Disassembled Cell

In Situ **Visualization**

The HTHP ABS Apparatus, now dubbed the HTHP Circulating System, had to be refitted with a cell that would safely sustain the target pressure of 20.7 MPa (3000 psia) and temperature of 121 ^{o}C (250 ^{o}F). The cell is shown in Figure 9. While commissioning tests of the HTHP Circulating

System have begun, a by-pass containing the Viewing Cell shown in Figure 4 will be added so that both ABS and optical imaging can be carried out at the same time.

Figure 9. New HTHP Circulating Cell

Pressure Transmissibility

A 20-ft length of ¼" stainless steel tubing fitted with pressure transducers at opposite ends was used for the initial tests to simulate a long fracture. The rate, as well as the amplitude, of pressure transmission of aphron-based drilling fluids was monitored. Later the transient measurements were replaced with steady-state measurements of pressure drop and change in pressure drop through the system as functions of the concentration of air.

To simulate flow through permeable media, sintered metal filters with various size pores were used initially. To enable flow visualization, a 92" length x 1" internal diameter clear PVC pipe was used in subsequent tests; the pipe was filled with sand of various grades and fitted with pressure transducers at the beginning and the end of pipe. The pipe was later shortened to 36". Packing of the pipe was accomplished various ways, including dry and in a fresh-water slurry. A photograph of the clear PVC apparatus is shown in Figure 10.

Figure 10. Clear PVC Pressure Transmissibility Apparatus

Aphron Shell Hydrophobicity

A literature search was conducted to determine appropriate methods for measuring the oil-wetting character of transient bubbles in various media under dynamic conditions. In addition, the theoretical basis for bubble and micellar agglomeration, coalescence and adhesion to to mineral surfaces was investigated.

A test method was proposed to measure directly the tendency for aphrons to stick together or to the walls of sandstone pores. A schematic of the apparatus is shown in Figure 11. A transparent APHRON ICS^{TM} mud sample is placed in the chamber of a syringe. The aphrons are filtered and compressed while driving the bulk fluid through a fine glass filter that prevents passage of the aphrons. The syringe is then back-filled with the same aphron-free fluid to its initial volume and the number of bubbles that have agglomerated, coalesced and/or stuck to the walls of the chamber are counted. This concept will be tested next Quarter.

Figure 11. Proposed Aphron Hydrophobicity Apparatus

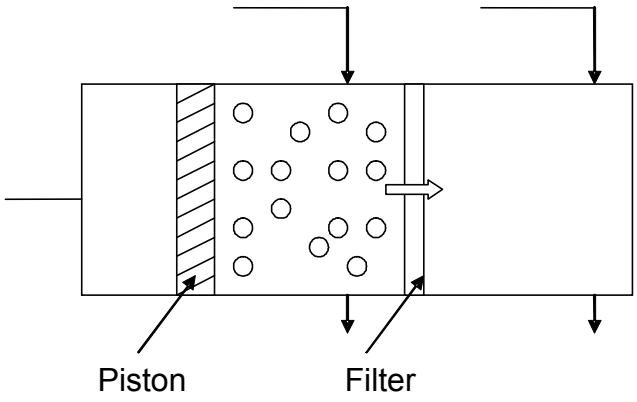

Sealing of Permeable and Fractured Media

These two projects utilize the same approach but with different types of porous media. A Core Leak-Off Test Apparatus was constructed that enables radial and axial loading of cores up to 6 inches in length, pressures up to 17.3 MPa (2500 psi) and temperatures up to 177 ^{o}C (350 ^{o}F). A schematic of this apparatus is shown in Figure 12:

Figure 12. Schematic of Leak-Off Tester

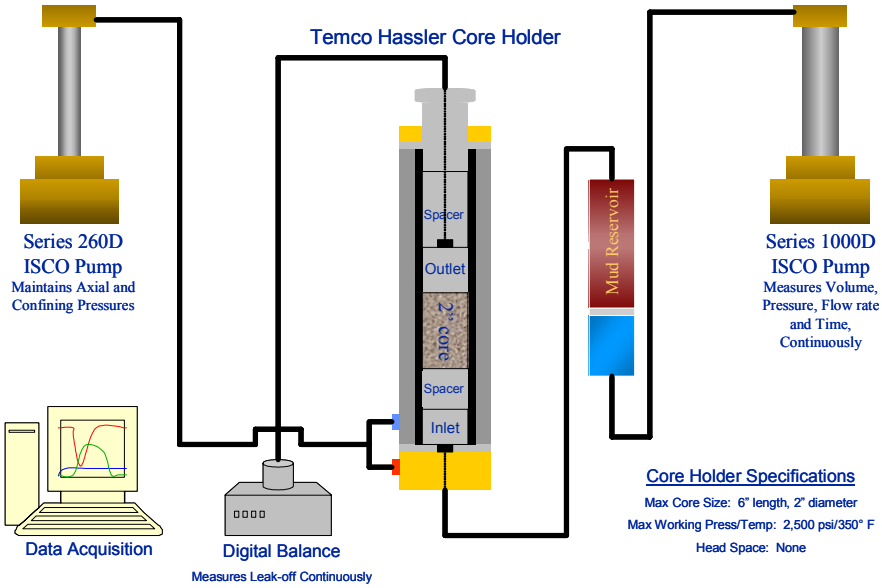

RESULTS AND DISCUSSION

Aphron Visualization

Acoustic Bubble Spectroscopy

Preliminary tests of the 3" x 3" hydrophones were run to determine how the units perform in water. They appear to be significantly more sensitive than the 1" x 1" hydrophones used previously, though the bubble size distribution (BSD) is still significantly skewed to much lower bubble sizes than we observe optically. The mean BSD determined with the ABS appears to be approximately 1/10 to 1/20 of the mean BSD determined optically. Furthermore, the minimum size recognized by the ABS software is 10 μm diameter, though one can usually make out bubbles optically that are considerably smaller.

The HTHP ABS Apparatus is nearing completion. Some modifications to the test cell are being made to improve safety, e.g. addition of handles, and a side stream is being added that will contain a viewing cell for optical imaging.

Optical Imaging

To determine the survivability of Aphrons above 7 MPa (1000 psig), as shown in last month's report, a sight flow glass cell, rated at 20.8 MPa (3000 psig), was obtained and used in experiments up to 13.9 MPa (2000 psig), the rating of the accumulator. A syringe pump was used to apply pressure through a 500-mL accumulator, which contains a floating piston that separates the hydraulic fluid (water) from the mud sample. A streaming video digital camera was used to capture the images of the mud as it underwent changes in pressure.

These tests were recorded using a streaming video digital camera and snapshots from the video are contained in this report.

In the first test, without magnification, the Transparent APHRON ICS™ mud was pressurized very quickly (<15 seconds) to 7 MPa (1000 psig) and then to 13.9 MPa (2000 psig). The 2000 psig pressure was maintained for 30 to 40 seconds and then reduced to zero. In the first photo in Figure 13, it can be seen that the aphrons block much of the fiber-optic light applied to the rear of the cell. The second photo shows transmission of a large amount of light due to the aphrons be-

ing compressed. The final photo of the series at the second zero psig indicates that the aphrons have returned to their original state.

The second set of photos (Figure 14) was recorded at 6X magnification using a microscope and the same sight flow glass cell which appears in the first set. A similar protocol was used from the previous test but an additional picture appears at the second zero plus 2.22 minutes. The sight glass was facing up, so that bubbles tended to accumulate under the viewing window. This test was the fourth pressurization of the same sample of Transparent APHRON ICS™ mud.

Figure 13. Transparent APHRON ICS™ Pressurized to 13.9 MPa (2000 psig): First Pressurization of This Sample

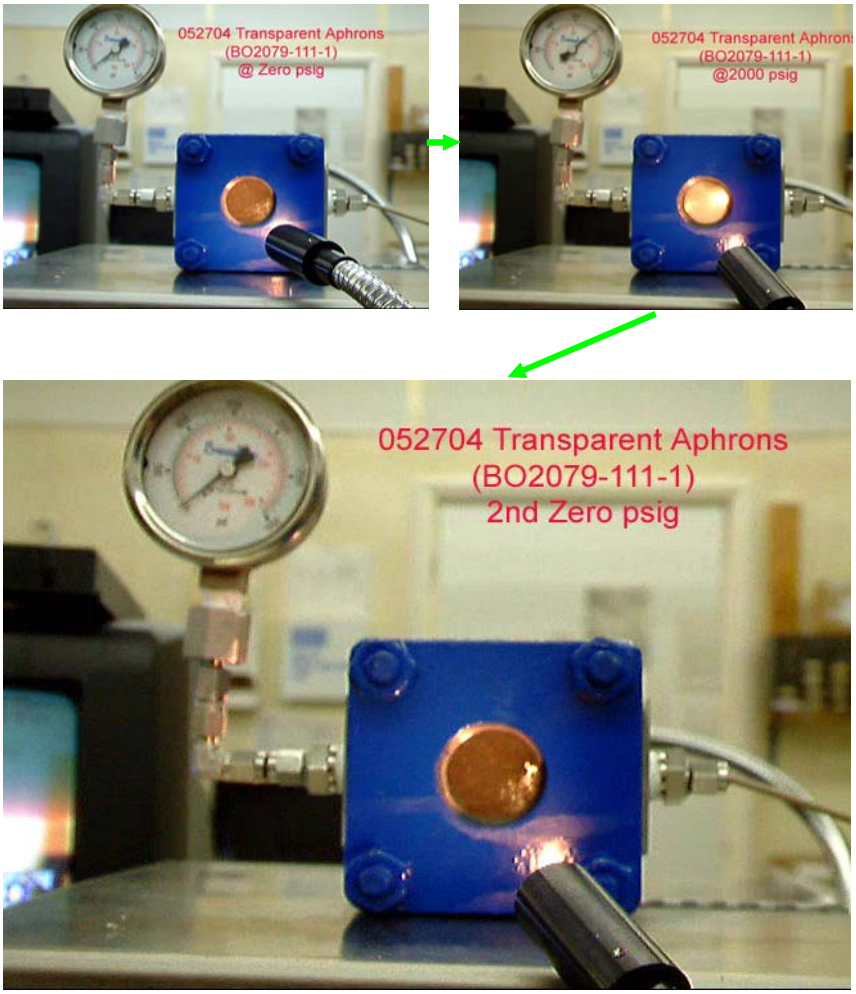

Figure 14. Transparent APHRON ICS™, Pressurized to 13.9 MPa (2000 psig): Fourth Pressurization of this Sample

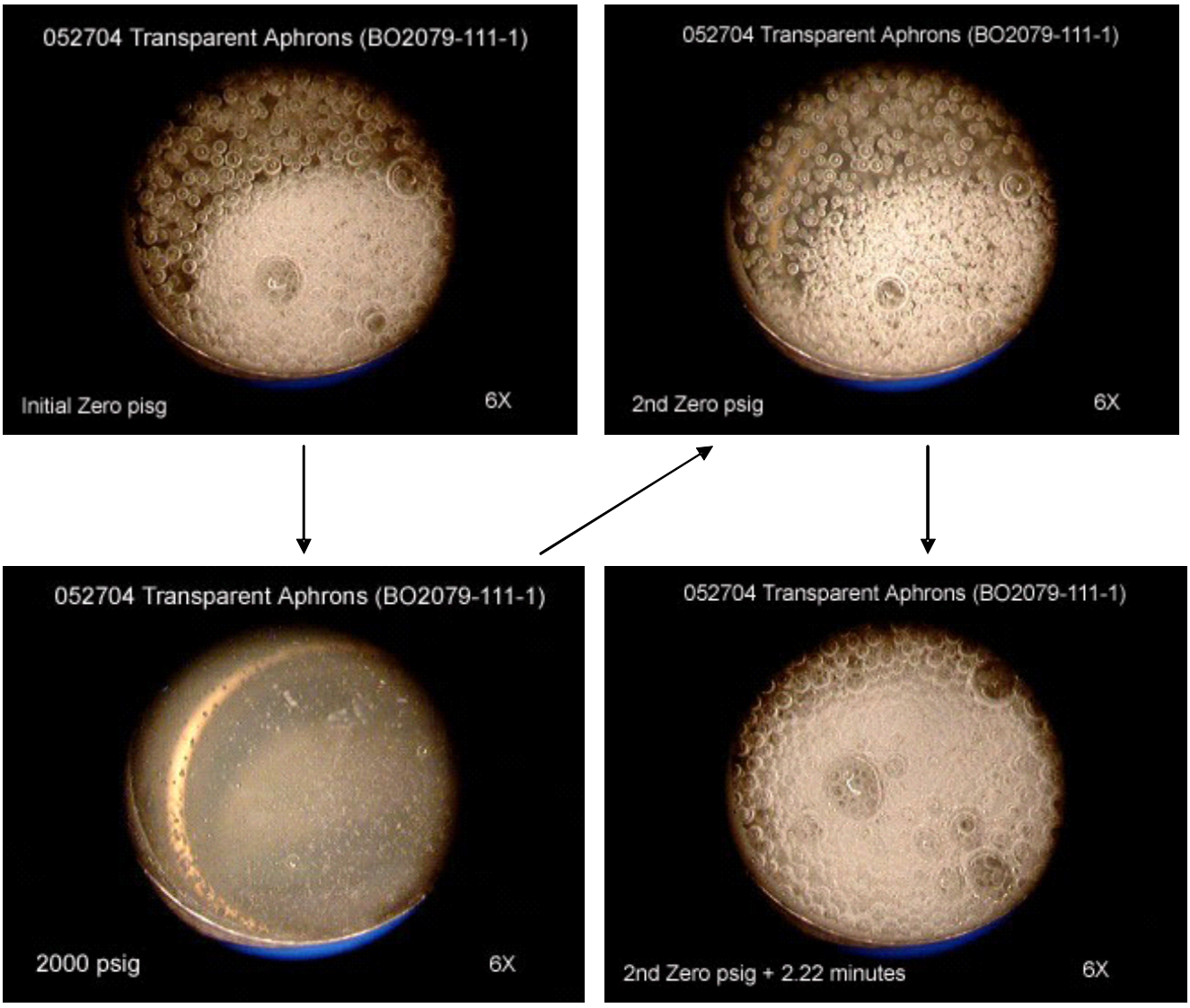

Conclusion: These tests indicate that Aphrons are stable to at least 2000 psig at ambient temperature. Immediately after depressurization (2nd Zero psig), the bubbles appear to be smaller than in their initial state (Initial Zero psig). However, after a couple of minutes (2nd Zero + 2.22 minutes), they have grown and appear to be larger than in their initial state. However, this is because some bubbles have been lost, very likely due to escape of air and dissolution into the sur-

rounding bulk fluid. When decompressed, the supersaturated fluid yields up its air into existing aphrons or forms new ones. Thus, it appears that there is a stability distribution among the aphrons: some remain stable to 2000 psig, while others do not. Modification of the formulation may reduce the incidence of poorly stable aphrons.

Another series of tests was conducted with the Transparent APHRON ICS™ mud up to 20.8 MPa (3000 psig), again using the glass viewing cell configured horizontally (Figure 15) and light entering only from the front. No magnification was used. The horizontal geometry is essential so as to minimize interference from "creaming" of the bubbles. In the first photo, at ambient pressure, the bubbles appear as a white "foam." When the mud was quickly pressurized to 20.8 MPa (3000 psig) -- second photo -- the fluid turned quite dark, inasmuch as the volume fraction of bubbles was greatly reduced. The pressure was maintained for 30 seconds, then reduced to zero and allowed to sit for a few minutes (third photo); this final photo at the second zero psig indicates that the bubbles have been regenerated as indicated by the re-appearance of the white foam.

The second series of tests carried out to 20.8 MPa (3000 psig) was made using a microscope, the same glass viewing cell as in the previous set (mounted horizontally) and the same mud sample (see Figure 16). The sample is first viewed at zero psig, using 15X magnification (photo #1). Then 20.8 MPa (3000 psig) is applied to the sample, and the magnification is increased to 40X (photo #2). Faint outlines of the bubbles at this pressure can be observed. The bubbles are faint because they have been driven deeper into the fluid and a good focus is not possible. The sample is depressurized 30 seconds later and the aphrons begin to expand (photo #3). Photo #4 shows the Aphrons at the 2nd Zero psig, 40X. Photo #5 shows the Aphrons at the 2nd Zero psig, 15X. It is clear that most of the bubbles (aphrons) survived pressurization to 20.8 MPa (3000 psig) and, consequently, they are regenerated essentially intact when depressurized to 0 psig.

Conclusion: These tests indicate that most of the aphrons this sample are stable to 20.8 MPa (3000 psig) at ambient temperature. When taken back down in pressure, they simply expand to their original size. Since the chemical composition of this fluid and the pressurization/depressurization scheme were the same as in the previous series of tests, one must conclude that after the first pressurization/depressurization, i.e. after the first test series, the bubbles had acquired a more stable configuration. Thus, the method by which the aphrons are generated is probably as important to the stability of the bubbles as the absolute chemical composition.

Figure 15. Transparent APHRON ICS™ Pressurized to 20.8 MPa (3000 psig): First Pressurization of this Sample

Figure 16. Transparent APHRON ICS™ Pressurized to 20.8 MPa (3000 psig): Second Pressurization of this Sample

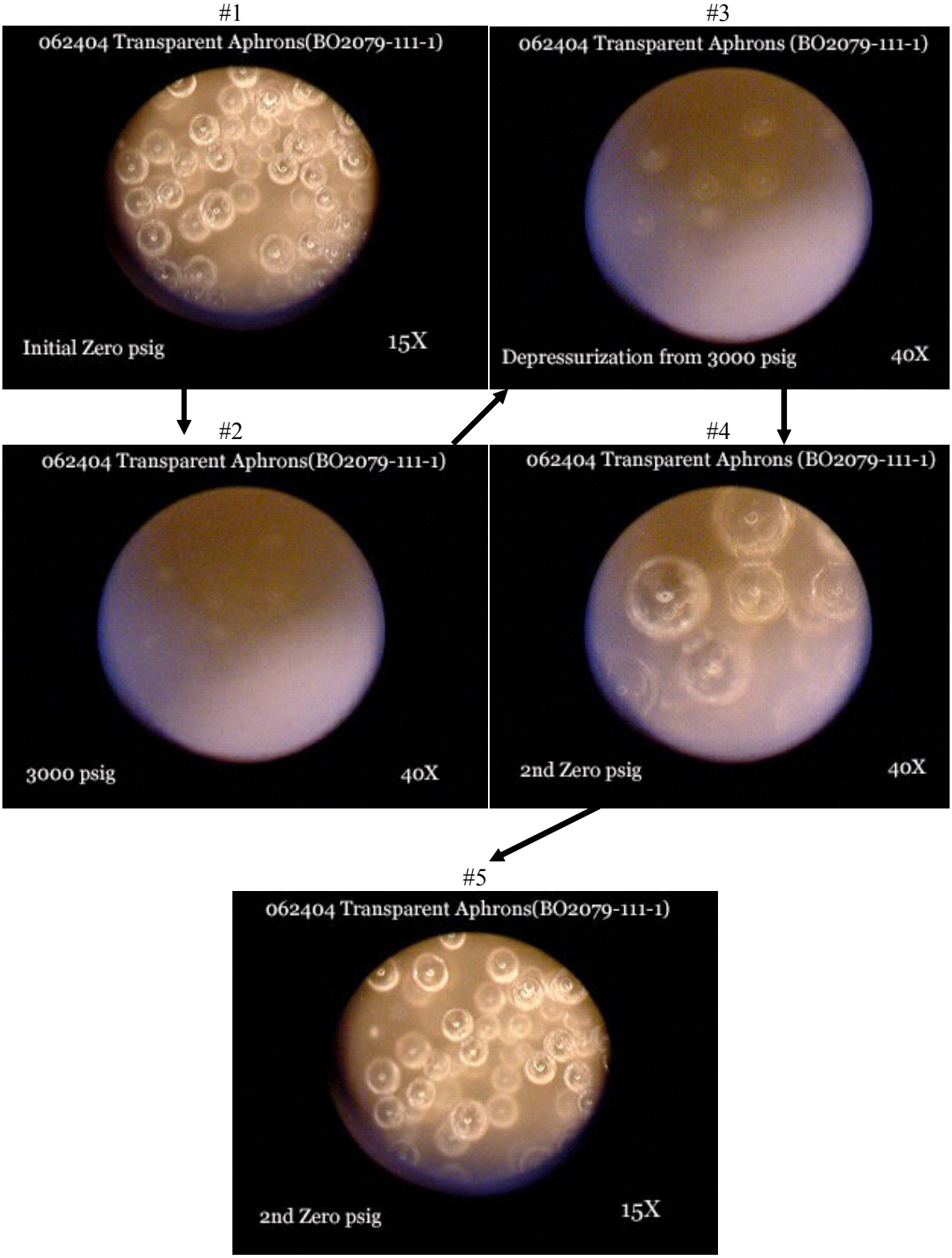

Fluid Density

A couple of examples of the compression/decompression data gathered with the Super Enhanced APHRON ICS™ mud are shown in Figures 17 and 18.

Figure 2. Fluid Density Test with Super Enhanced APHRON ICS™ Mud Sample #1

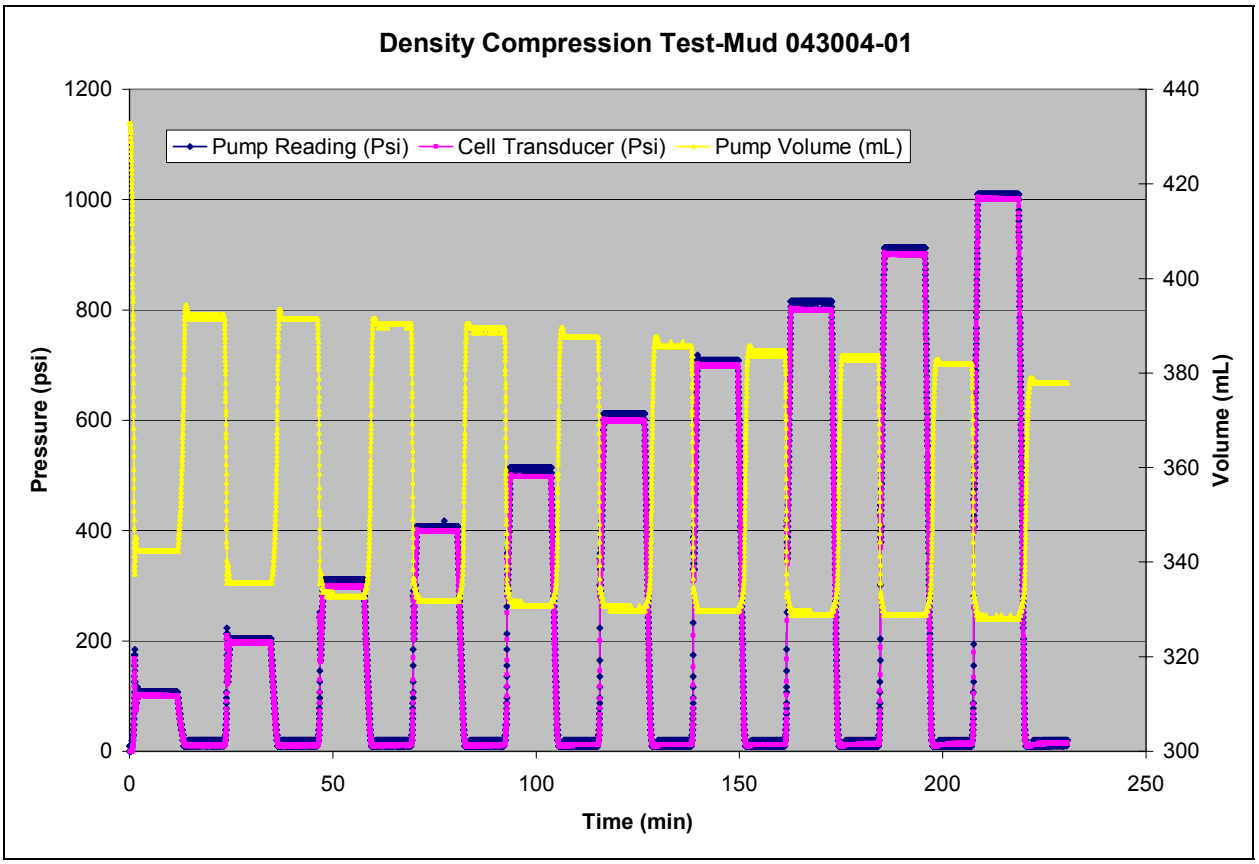

Figure 18. Fluid Density Test with Super Enhanced APHRON ICS™ Mud Sample #2

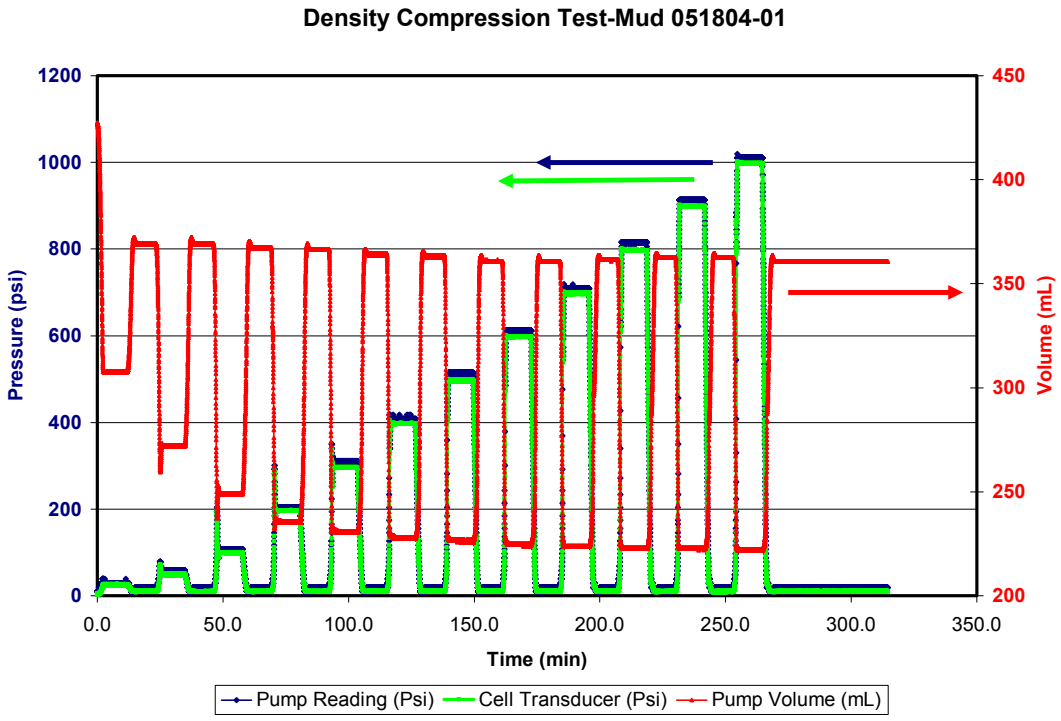

When the system is depressurized, it is assumed that air solubilized during a previous pressurization step requires significantly more time to come out of solution than air trapped within aphrons. Thus, the steady-state volume recovered after each depressurization step represents aphrons that retained their integrity during the previous pressurization step. Since there is some uncertainty in the position of the piston during the initial application of pressure to the system, the reference point is chosen to be the first depressurization step, i.e. after the 100-psig step in Figure 17 and after the 25-psig step in Figure 18; this is assumed to represent 100% volume recovered (100% of the aphrons survive). All subsequent recovered volumes are compared to this volume. It should be noted that the pump pressure during the depressurization step does not drop to 0 psig, rather about 10 psig (again due to the stick-slip phenomenon mentioned in the Experimental Approach). Each post-pressurization volume measurement was made at that same pressure of 10 psig.

In the examples above, the amount of entrained air in the mud initially had been calculated from density measurements. However, this can be determined more accurately from the compressibility data. Applying the Ideal Gas Law, PV = nRT, for a fixed number of moles of air, n, at a constant temperature T, the product of pressure and volume, PV, should be constant. Thus, when a gas is compressed from P_1 to P_2, the change in volume from V_1 to V_2 should compensate exactly to give $P_1V_1 = P_2V_2$. This is illustrated in Figure 19 by the horizontal red line. The mud sample used in the data presented in Figure 18 nominally contained 55% air by volume. However, one can see that with 55% air, PV increases with increasing pressure. Through trial and error, one can determine that if the initial amount of air had actually been 49%, PV would remain constant throughout the test. Thus, it is concluded that 49% air is a more accurate value for the initial concentration of air in the mud at ambient pressure.

Figure 19. Determination of % Entrained Air in Fluid

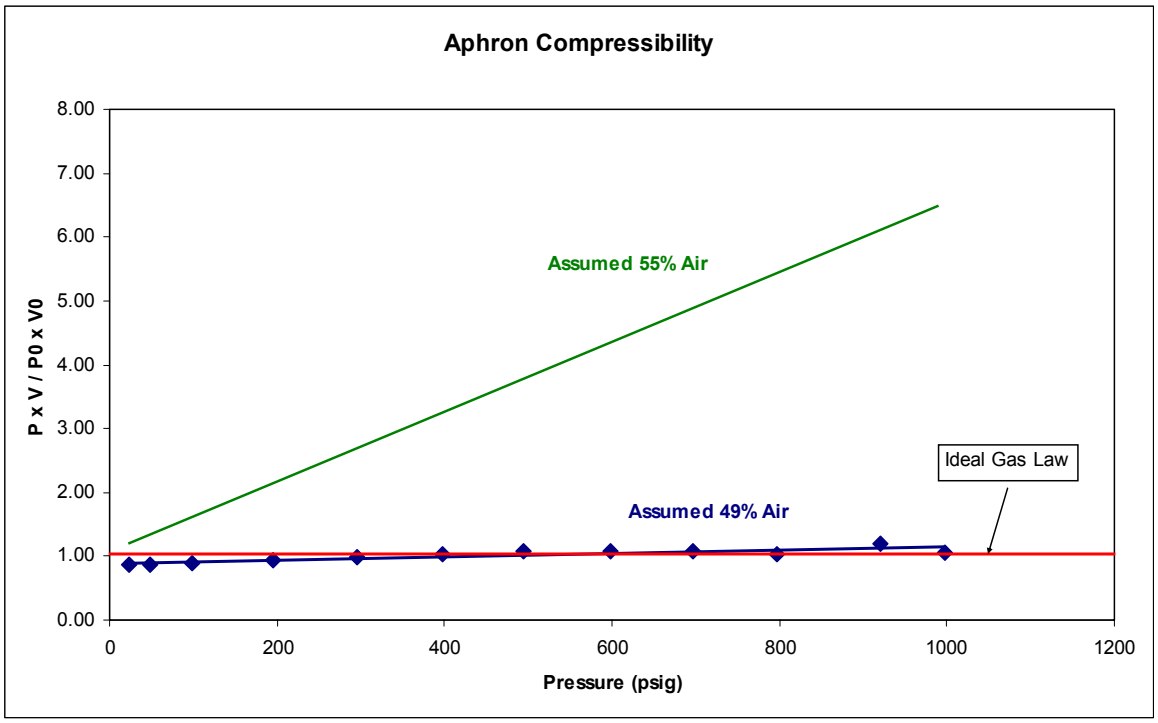

Analysis of Figures 17 and 18 indicates that, with increasing pressure, less and less volume is recovered when the system is depressurized, which we interpret as air which is lost from the aphrons and has gone into solution. However, the fraction of aphrons that is lost is relatively low, as shown in Figure 20. Here the data used was the set shown in Figure 18. The fraction of aphrons that survive after each depressurization step is given by

$$P^*(V_{cell} - V_{0fluidcell})/P_0^*V_{0aircell}$$

where P_0 is the absolute pressure and $V_{0aircell}$ the volume of air at the beginning of the test series; P is the absolute pressure and $V_{cell} - V_{0fluidcell}$ is the volume of air after each subsequent pressurization/depressurization step. $V_{0aircell}$ was 49%, as determined from the procedure described above. As shown in Figure 20, it is evident that essentially all of the aphrons (> 95%) survived pressurization up to 7 MPa (1000 psig). This is consistent with the aphron visualization tests described in the previous section.

Figure 20. Effect of Pressure on Aphron Survival

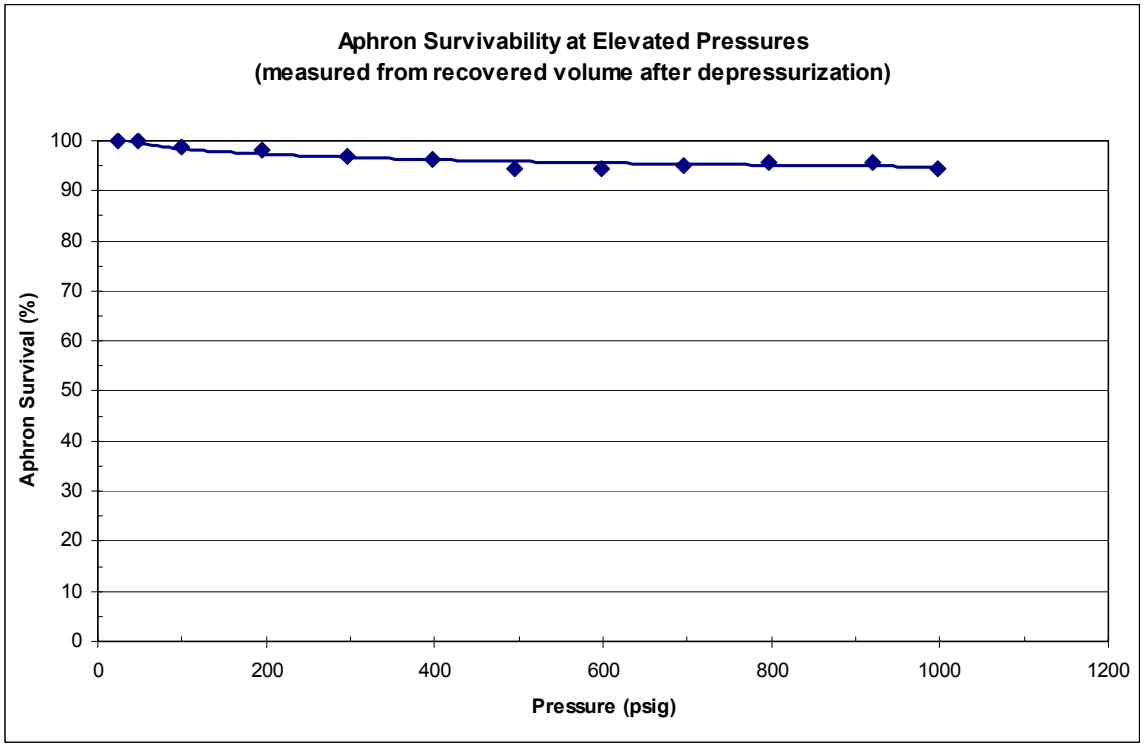

Aphron Air Diffusivity

The FOXY T-1000 fluorescence quenching probe (Ocean Optics) was shown to be unacceptably delicate (the manufacturer was not able to keep the silicone coating from peeling off) and gave incorrect values of dissolved oxygen (DO) in high-viscosity fluids, such as the APHRON ICS™ drilling fluid. Other DO probes were examined. The one that proved to be the most reliable was a Hach SC100 (see Figure 21). This particular probe is a break-through technology that relies on a timed response to an LED signal. Although this probe cannot be used at pressures above 20 psig and is limited to only moderate temperatures, initial tests showed it to be rugged and to give a fast response time.

Tests were ran with the Hach SC100 under ambient conditions to determine the effects of (a) type of drilling fluid, (b) low-shear-rate viscosity and (c) aerobic biodegradation. For this purpose, a variety of different drilling fluids, some containing varying levels of viscosifier and biocide, were run to elucidate whether the rate of loss of air from aphrons could be determined by monitoring the concentration of dissolved oxygen.

Figure 21. The Hach SC100 DO Probe

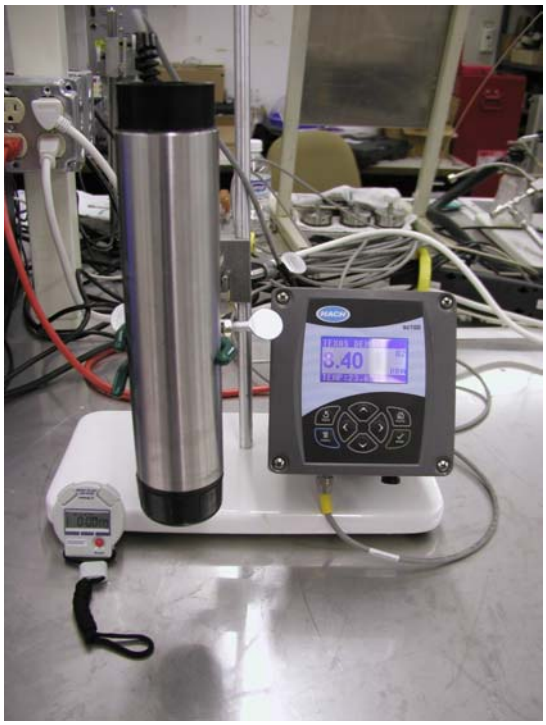

The Hach SC100 showed very encouraging results. Response time was rapid, generally giving a steady-state value of DO within 15 to 30 min, depending on viscosity and how the probe was introduced into the sample. As shown in Figure 22, the steady-state DO values recorded for the Super Enhanced (SE) APHRON ICS™ mud dropped very quickly. Indeed over the initial 3-hr period between mixing the mud and getting a steady-state DO reading, the concentration of DO had already dropped by more than 50%. Initial readings were approximately 8.5 ppm. As shown in Figure 22, a 30-ppb slurry of Black Hills bentonite retained that value indefinitely. Apparently the Transparent APHRON ICS™ mud, which lacks the hemicellulose, starch, MgO and EMI-802 of the regular SE APHRON ICS™ mud, also remained high, at least for the first couple of days. But the regular SE APHRON ICS™ mud depleted DO very rapidly, so that within a day the concentration of DO was negligible. This system contains a low level of X-CIDE, a powerful biocide.

Xanthan gum, one of the main components of the APHRON ICS™ mud system, can undergo aerobic biodegradation, but the process is thought to be relatively slow. Tests here indicate that when long-term DO monitoring tests were conducted of a pH-adjusted solution of xanthan gum, here in the form of a premium grade called FloVis Plus, DO did indeed fall, though not as rapidly as it did in the SE APHRON ICS™ mud system. The FloVis Plus solution did not contain any biocide. Thinking that aerobic biodegradation might be involved in the depletion of DO in the SE APHRON ICS™ mud, the level of X-CIDE was increased from 0.1 to 5 ppb. As is apparent in Figure 22, even with 5 ppb X-CIDE, the depletion rate of DO was not affected significantly. It appears, therefore, that some of the components in the SE APHRON ICS™ system cited above, namely the hemicellulose and starch, are very likely reacting directly with dissolved O_2. This process is so rapid -- and in all likelihood is even more rapid at elevated pressures and temperatures -- that it is not possible to use DO as an indicator of the diffusion rate of air from aphrons.

Similar long-term exposure tests were run with other fluids, as shown in Figure 23. While the EMS-2100 (clay-based APHRON ICS™) and 3% KCl FloPro NT systems (with biocide) did not show any indication of a drop in DO over time, DrilPlex (an inorganic polymer containing an organic fluid loss control agent) did exhibit a steady drop in DO, though not as rapid as FloVis Plus without biocide.

Figure 22. Effect of Time on DO Concentration in Various Drilling Fluids

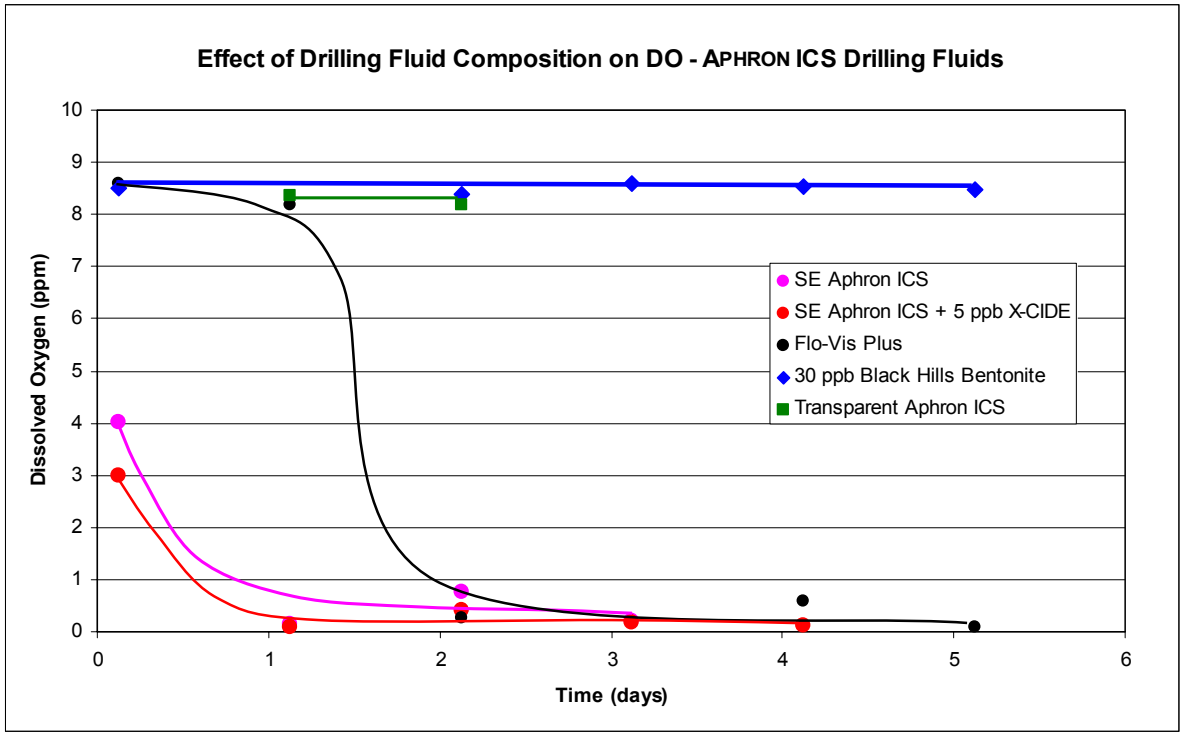

Figure 23. Effect of Time on DO Concentration in Miscellaneous Fluids

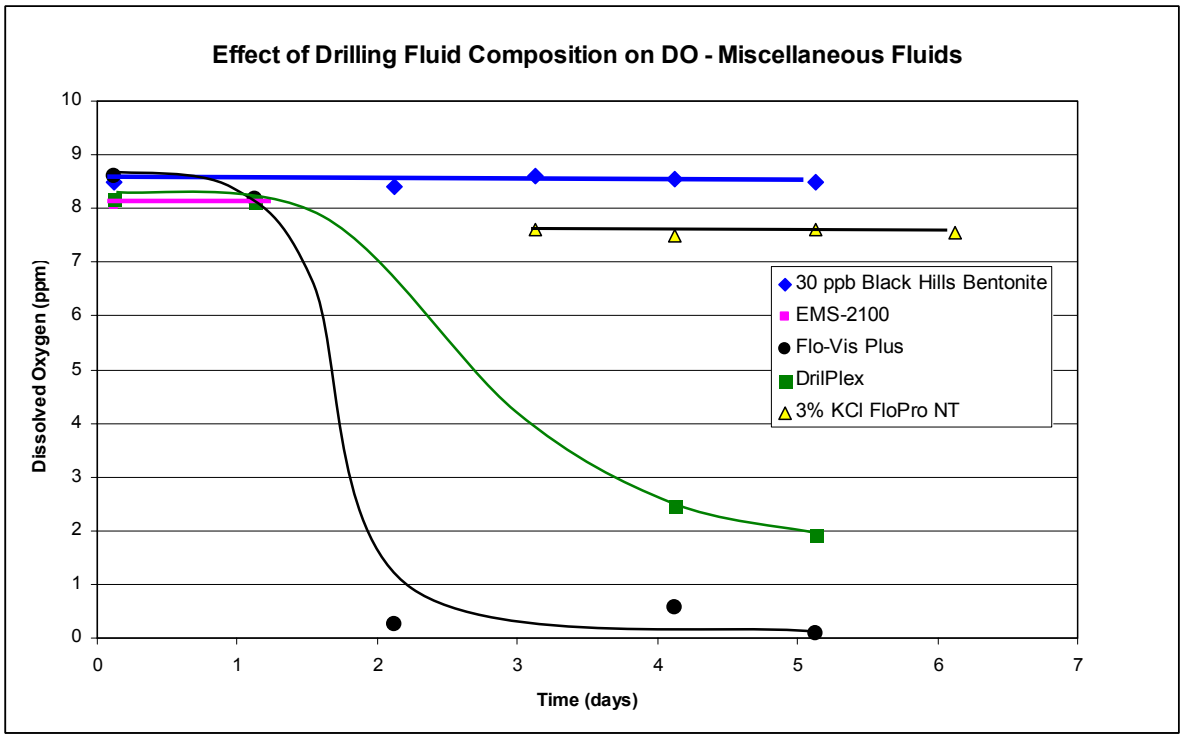

Little or no effect on the steady-state value of DO was observed due to viscosity; even the rate of attainment of the steady-state value of DO was not slowed much by high viscosity.

The effect of LSRV on steady-state DO was determined using freshly prepared solutions of FloVis Plus (with different concentrations of FloVis Plus) that ranged in viscosity from 97 kcP to 156 kcP. The steady state DO in all cases ranged from 8 to 8.5 ppm.

Some of the SE APHRON ICS™ muds have been prepared with 2 ppb Blue Streak, while others employed 1 ppb of the aphron generator. There has been some concern that the higher concentration of Blue Streak might affect some of the properties of mud, including viscosity and perhaps DO. Thus, tests were conducted with concentrations of Blue Streak varying from 0.5 to 3 ppb. The results are shown in Figure 24. No apparent change in LSRV was noted for deaerated samples of the mud. When air was introduced, however, LSRV appeared to drop significantly at concentrations of Blue Streak above 1 ppb. This has not been confirmed, and it is not known what other effects may result from using higher-than-normal concentrations of Blue Streak. In the near future, however, all "standard" APHRON ICS™ mud samples will be prepared with 1 ppb Blue Streak.

Figure 24. Effect of [Blue Streak] on LSRV

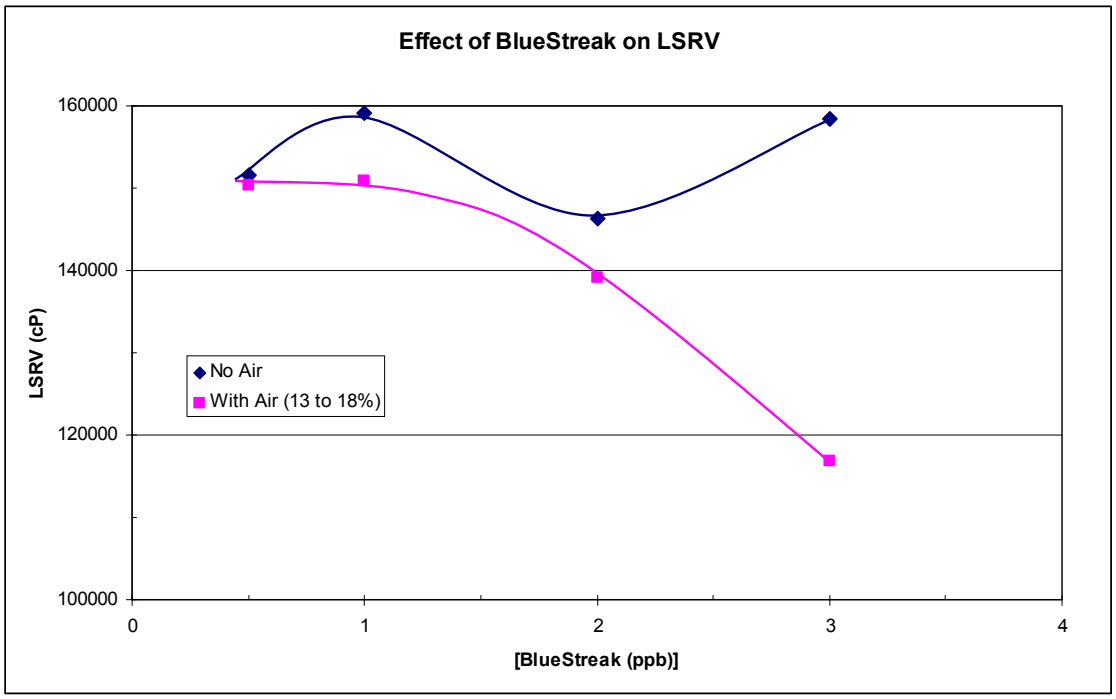

Thus, although viscosity is not a problem and aerobic biodegradation can be controlled, some components of the Super Enhanced APHRON ICS™ mud appear to serve as substrates for direct oxidation. This leads to inescapable conclusion that, even at ambient pressure and temperature, DO reacts with these components so rapidly that monitoring of DO is not an acceptable method of measuring the rate of loss of air from aphrons.

The focus has now turned to monitoring the rate of change of bubble size as a function of pressure and temperature. This had been the method of choice originally for determining the rate of loss of air from aphrons, but at the time, there were instrumentation issues that precluded use of this method. Now we have a transparent cell that will permit monitoring the size of even a handful of bubbles as a function of pressure, up to as much as 27.7 MPa (4000 psig).

Pressure Transmissibility

Filtration through 2-μm and 7-μm Swagelok™ Sintered Metal Filters

Samples of a Transparent APHRON ICS™ mud -- with aphrons and without aphrons (after centrifugation) -- were used for experiments with the sintered metal filters. Two different procedures were use for these experiments:

a. Initially 0.7 MPa (100 psig), 150 or 200 psig was applied to the mud in an accumulator, then the valve was opened to permit mud to flow through a filter at a constant rate of 50 mL/min.

b. No pressure was applied to the mud initially, and the experiment was conducted as above with a constant flow rate of 50 mL/min.

The results of these two sets of experiments are summarized below, using a 2-μm filter:

Figure 25. Flow of Transparent APHRON ICS™ Mud through 2-µm Filter

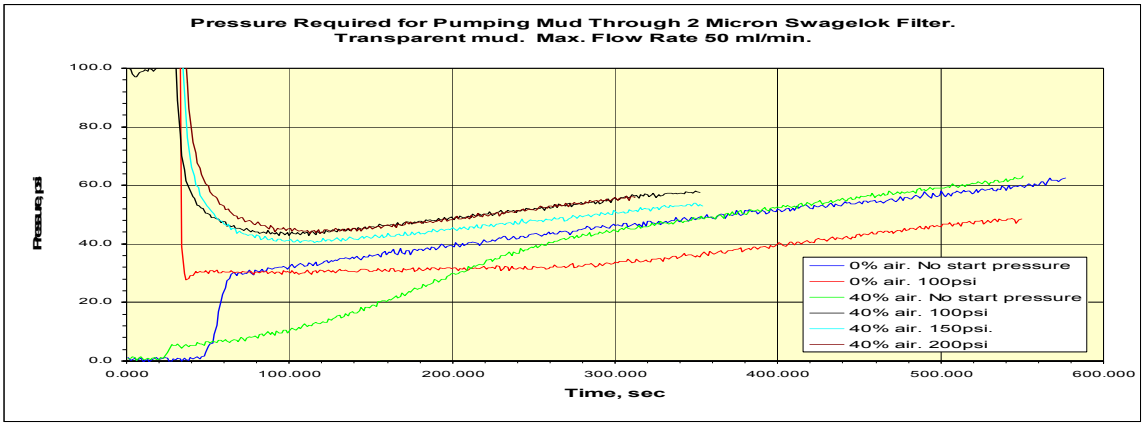

Figure 26. Flow of Transparent APHRON ICS™ Mud through 10-µm Filter

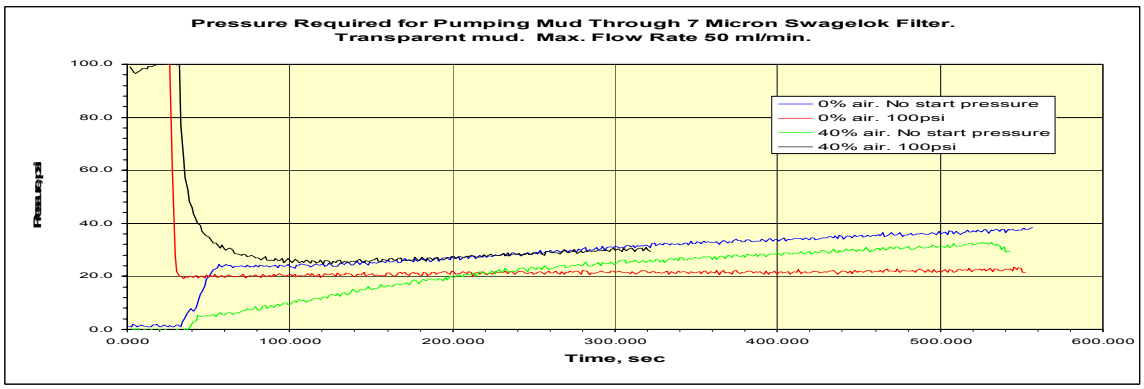

Only 35-50 psi and 20-35 psi of pressure was required to pump the mud through 2-µm and 7-µm filters, respectively, at a flow rate of 50 mL/min. These results appeared to be independent of aphron concentration and method of running the tests, and thus are attributable to the base fluid itself. Pressure increased linearly with time and with about the same slope. This was the case for all of the aerated samples as well as the regular deaerated samples; the pre-pressurized deaerated samples proved to be exceptions, showing no increase in pressure with time, at least for awhile. The increase in pressure with time is associated with plugging or with an increase in the length of the mud column, i.e. as if mud occupied a longer and longer portion of the tube on the back side of the filter. However, this section of tubing is only a few centimeters in length, and mud occupied all of that volume within a few seconds of the start of each test. Thus, although

these samples are nominally "solids-free" (this is the Transparent formulation), the increase in pressure drop must be due to plugging of the filter.

The aphron-laden samples that were pre-pressurized to 100, 150 and 200 psig (100 psig = 0.7 MPa) exhibited a higher resistance to the flow through the 2-μm filter than did the aphron-free mud. This effect was not observed with the 7-μm filter. Furthermore, when the system was not pre-pressurized to 100 psi, no difference were observed in the pumping pressure of the two muds using the 2-μm filter and just a small difference using the 7-μm filter. The 10-12 psi pressure difference observed between the two samples in the pre-pressurized tests must be due to a difference in the size distribution of the air bubbles that results from pressurization and depressurization. When the system is not pre-pressurized, the aphron mud appears to compress to the point where the bubbles do not affect the pressure drop at all.

Sand Packs in Clear PVC tubing:

20/40 and 70/100 mesh sand were used for preparation of sand packs. Two series of experiments were conducted with each size of sand. In the first series, water-filled sand packs were blown with air to drive excess water from the sand pack yet leave the sand water-wet. In the second series, the sand packs were filled with water at the beginning of the experiment and tested in that state. Additional experiments were conducted with 20/40 and 70/100 mesh dry sand.

The results of all the sand pack experiments are shown in Figures 27-31.

As is shown in Figures 27 and 28, the APHRON ICS™ mud sealed both sizes of water-wet sand packs. The pressure drop across the sand pack was 45 to 55 psi for the 20/40 sand and 85 to 95 psi for the 70/100 sand (100 psi = 0.69 MPa). This follows conventional wisdom. On the other hand, the effects of aphrons on pressure drop in the water-wet sand packs are not entirely consistent. The results summarized in Figures 27 and 28, for example, show that in the 20/40 sand pack the aerated mud (18% air) generates a pressure drop that is about 8 psi higher than the centrifuged mud (0% air), as expected, but in the 70/100 sand pack the aerated mud (25% air) generates a pressure drop that is about 16 psi lower than the centrifuged mud.

Figure 27. Flow of Transparent APHRON ICS™ Muds through 20/40 Sand Pack

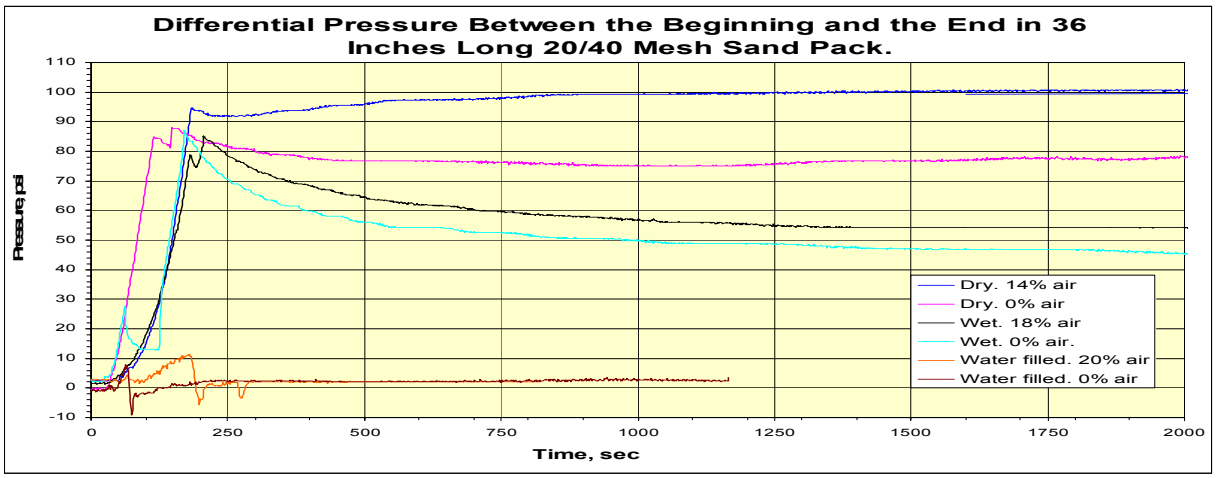

Figure 28. Flow of Transparent APHRON ICS™ Muds through 70/100 Sand Pack

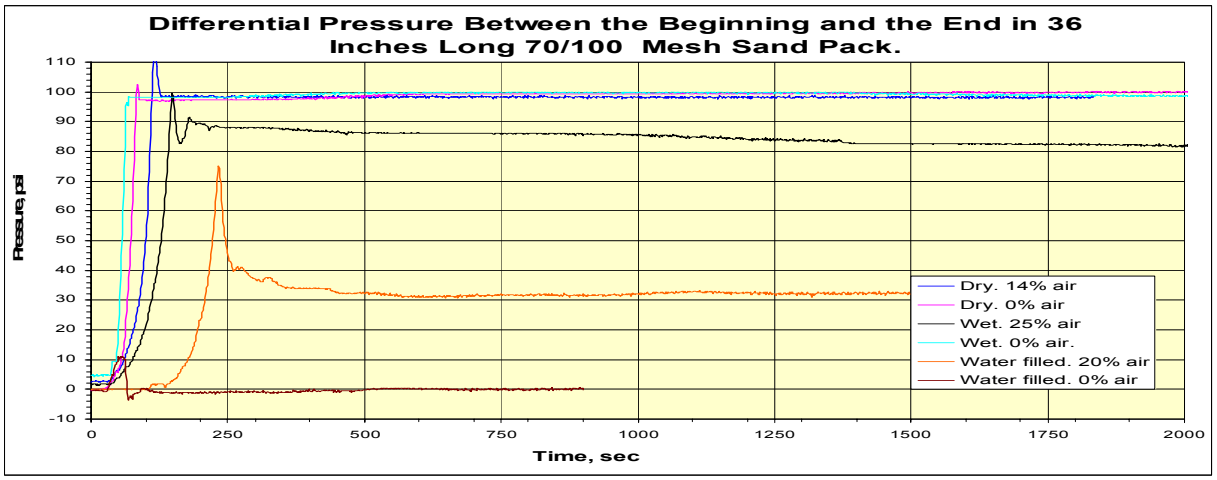

The results of additional experiments with water-wet sand packs verified this erratic and difficult-to-reproduce behavior. The surface condition of the sand in the water-wet sand packs was different every time. Flushing of the excess water from the sand bed, yet leaving all surfaces water-wet, was not completely successful, inasmuch as the back end of the bed tended to be much drier than the front end. This can explain the poor reproducibility of the collected data.

The Leak-Off test results for dry sand packs were a little different for 70/100 versus 20/40 mesh sand. In both cases, the APHRON ICS™ mud effectively sealed the dry sand packs and no filtrate was collected after 30 minutes. In the dry 20/40 mesh sand, the centrifuged mud (0% air) produced a pressure drop of about 77 psi, while the mud containing aphrons (14% air) produced a pressure drop of 100 psi. In the dry 70/100 mesh sand, on the other hand, both muds produced about 100 psi pressure drop. The procedure for preparing the dry pack did not change the character of pressure transmission, but it did change the depth of penetration of the mud. One experiment was conducted by filling the pipe with wet slurry of 70/100 mesh sand, followed by complete drying using air and nitrogen. The differential pressure established across this sand pack was almost 0 psi for the mud containing 18% air and similar to the sand pack filled with dry sand, but invasion of mud inside the previously wet (but dried) sand pack was about 3 times higher. This difference in the behavior of these dry sand packs could be explained by change of the condition of the sand pack, due to development of a water film attached to the surface of sand after it was wetted and which may have survived during the air/nitrogen drying process.

When the sand packs were completely filled with water at the beginning of the tests, pressure transmission took on a different character. The results are shown in Figures 29-31. High pressure from the pump propagated very fast in sand packs filled with water. The differential pressure established across 20/40 sand packs was almost nil in muds containing 0% and 20% air. For the 70/100 sand packs, however, a consistent difference was observed for aerated muds compared to deaerated muds. As is shown in Figures 29-31, muds with 0% air showed 10-30 psi less pressure drop than muds containing 13 to 22% air. Also, both the filtration rate and the rate of change of the filtration rate were lower for aerated muds than for deaerated muds.

These experiments show that both pressure transmissibility and invasion of aphron muds in a sand pack depend heavily on the packing method and the presence of water in the sand pack. Compared to dried or wet sand packs, which have high void volumes, invasion of mud in water-filled sand packs was very small in all cases. In addition, for the lower permeability water-filled sand pack (70/100 sand), pressure transmissibility and depth of invasion are reduced significantly by aphrons in the mud. Downhole, sands are most likely filled with water; consequently, the experiments with dried sand packs and wet sand packs have been discontinued, and all subsequent tests will be conducted with water-filled sand packs.

Figure 29. Pressure Drop for Transparent APHRON ICS™ Fluids in Water-Filled 70/100 Sand Pack

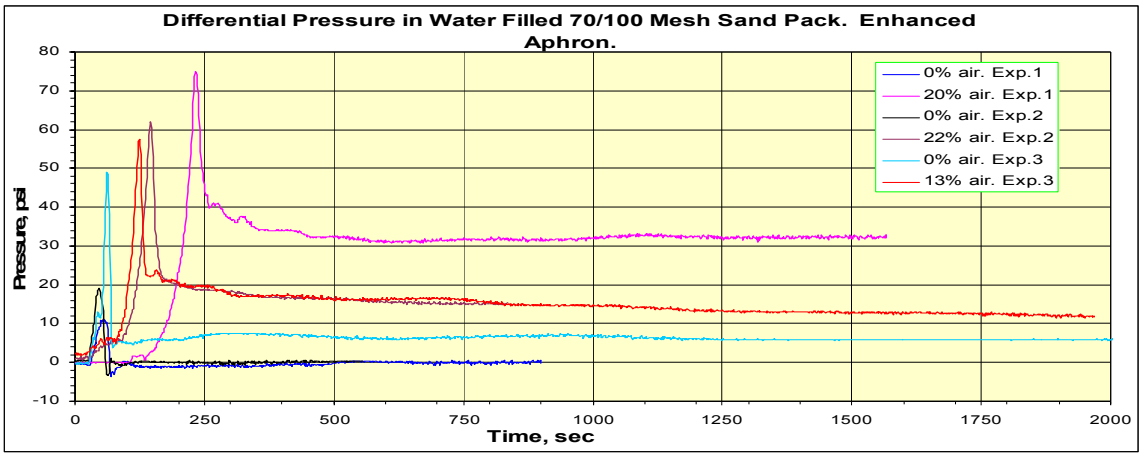

Figure 30. Filtration Rate for Transparent APHRON ICS™ Fluids in Water-Filled 70/100 Sand Pack

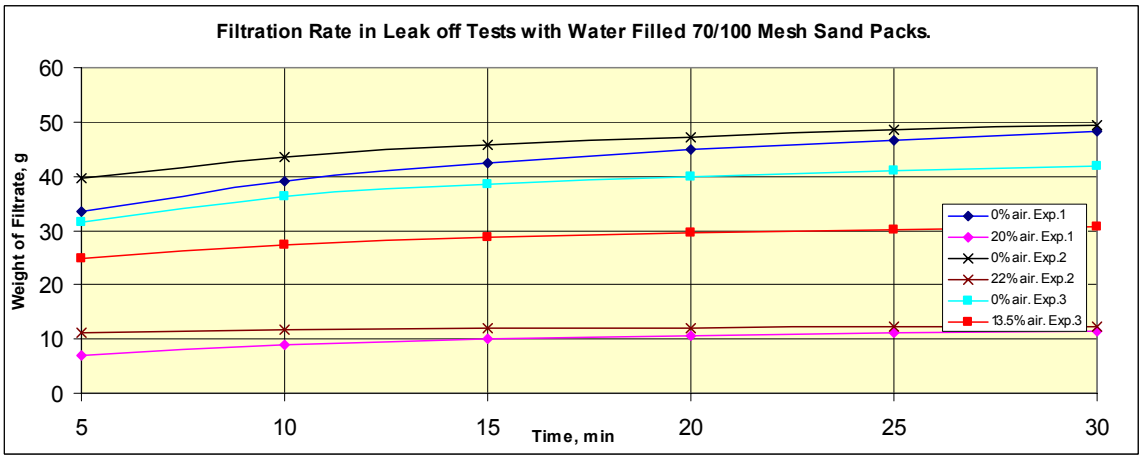

Figure 31. Change in Filtration Rate for Transparent APHRON ICS™ Fluids in Water-Filled 70/100 Sand Pack

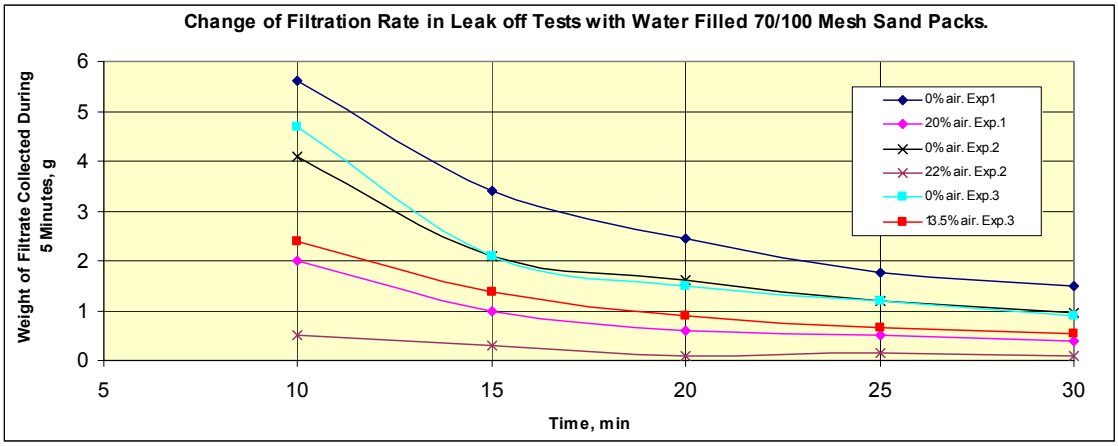

Water Permeability of 20/40 and 70/100 Mesh Sand Pack:

An ISCO pump connected to an accumulator and a water column to generate a constant hydro-static head were used to generate a constant flow rate of water through the 70/100 and 20/40 mesh sand packs. The permeability of the sand packs was estimated using the Darcy equation, which relates the volumetric flow rate to the pressure drop, viscosity, cross-sectional area and length of the packed tube:

$$Q = -\frac{\kappa A}{\mu}\left(\frac{dP}{dx}\right)$$

Q = Volumetric Flow (cm^3/s)

k = permeability (Darcy, $(cm^2*cP)/(s*a^{TM})$)

A = cross-sectional area, 4.37 (cm^2)

μ = viscosity, 0.89 at 26^0C (cP)

P = pressure (a^{TM})

X = length, 91.44 (cm)

Thus, $$k = 18.6\frac{Q}{\Delta P} \text{ in Darcy}$$

The results of the permeability determinations are shown in the Table 1.

Table 1. Water Permeability of Sand Packs

	70/100 mesh sand pack			20/40 mesh sand pack		
Experiment	Q, mL/min	P, a^{TM}	k, Darcy	Q, mL/min	P, a^{TM}	k, Darcy
1	0.33	0.73	8.4	0.54	0.11	91.3
2	0.31	0.71	8.1	0.55	0.10	102.3
3	0.29	0.62	8.7	0.54	0.10	100.4
4	0.32	0.74	8.0	0.53	0.10	98.6
Average:			8.3			98.2

The significant difference in permeability of 20/40 and 70/100 sand packs strongly affects the ability of aphrons to influence depth of fluid invasion and pressure transmissibility.

Aphron Shell Hydrophobicity

Based on an initial survey of the literature, measurements of interfacial tension and contact angle would be sufficient to describe the oil-wetting nature of aphrons. With that in mind, Kreuss brought in a demo model of a BP2 Bubble Pressure Tensiometer to determine its suitability for measurements of surface tension and interfacial tension in the APHRON ICS^{TM} mud system. Unfortunately, it appears that the very high LSRV of the system precludes getting usable steady-state measurements of the surface tension.

The search for a suitable method to measure contact angle of bubbles narrowed to Contact Angle Goniometry. Rame-Hart offers such a device. For this method to provide usable information, it is necessary to construct a device to apply compressive and/or shear stresses on the bubbles while measuring contact angle.

While the contact angle method is promising and will be looked at in more detail, attention is now focused on measurements of the net oil-wetting character of aphrons by measurements of rate of agglomeration and coalescence of the aphrons and strength of adhesion of aphrons to mineral surfaces under compressive and/or shear stresses.

A test method is proposed to measure directly the tendency for aphrons to stick together or to the walls of sandstone pores. A schematic of the apparatus is shown in the Experimental Approach. Conceptual data are being gathered using a syringe fitted with frits of well-defined pore sizes.

Sealing of Permeable and Fractured Media

Various components of a triaxial loading core leak-off tester have been acquired from Temco. An oven has also been purchased and has now been installed. The first Leak-Off tests in the new coreholder will be conducted during the next Quarter.

CONCLUSIONS

Because the Acoustic Bubble Spectrometer (ABS) yields Bubble Size Distributions (BSD) in aphron drilling fluids that are erroneously low by at least an order of magnitude, yet does not recognize bubbles smaller than 10 μm diameter, we will need to rely on photomicrographic (optical) measurements of BSD. A variable-reservoir-depth viewing cell promises to be useful for that purpose, even for opaque fluids. Nevertheless, the HTHP Circulating system, which is nearing completion, will utilize both ABS and an optical viewing cell for observations of aphrons. In addition, the Environmental Scanning Electron Microscope appears to be ready for high-magnification examination of aphrons *in situ*.

Repeated compression / decompression of aphrons reveals that aphrons can survive pressures up to at least 3,000 psi. Up to pressures of 1,000 to 2,000 psi, essentially all aphrons survive repeated compression and decompression. Above that pressure, however, many smaller aphrons disappear during compression; on decompressing, the number of bubbles is significantly reduced and the survivors are larger. This growth process requires a few minutes to reach a steady state. There is some evidence also, that some aphrons can withstand compression better than others, depending on composition of the mud. In particular, aphrons in the Transparent APHRON ICS™ mud, which lacks some key components, appear to follow the Ideal Gas Law more closely than aphrons in the Super Enhanced APHRON ICS™ mud.

Monitoring of dissolved oxygen has proven to be unsuitable for determination of the kinetics of air loss from aphrons, because some components in the drilling fluid react very rapidly with dissolved oxygen. Thus, direct optical imaging of the fluid is being used to achieve that objective.

Lastly, it was found that the base fluid in APHRON ICS™ fluids gives significantly larger pressure loss in long conduits and permeable sands than does any other conventional high-viscosity drilling fluid. Furthermore, in permeable sands, aphrons move ahead of the liquid stream, enabling them to form a partial seal, slowing the rate of fluid invasion even more and increasing the pressure drop across the sands.

REFERENCES

1. Growcock, F. B., Khan, A. M. and Simon, G. A.: "Application of Water-Based and Oil-Based Aphrons in Drilling Fluids," SPE 80208, presented at the SPE International Symposium on Oilfield Chemistry, Houston, Texas, Feb. 5–8, 2003.
2. Sebba, F.: *Foams and Biliquid Foams – Aphrons*, John Wiley & Sons Ltd, 1987.
3. Chahine, G. L. and Kalumuck, K. N., "Development of Near Real-Time Instrument for Nuclei Measurement: The ABS Acoustic Bubble Spectrometer," Proc. FEDSM'03, International Symposium on Cavitation Inception, 4th ASME_JSME Joint Fluids Engineering Conf., Honolulu, Hawaii, July 6-10, 2003.

LIST OF ACRONYMS AND ABBREVIATIONS

ABS = Acoustic Bubble Spectroscopy

APHRON ICS™ = Aphron Invasion Control System

Blue Streak = Surfactant package that serves as aphron generator for the APHRON ICS™ system

BSD = Bubble Size Distribution

DO = Dissolved Oxygen

EMI- = Experimental M-I *LLC* product

FloVis Plus = Xanthan Gum polymer

HTHP = High Temperature and High Pressure

OD = Outer Diameter

PVC = polyvinyl chloride

SE = Super Enhanced